

Adaptive target birth intensity for PHD and CPHD filters

B. Ristic^a, D. Clark^b, Ba-Ngu Vo^c, Ba-Tuong Vo^d

Abstract

The standard formulation of the PHD and CPHD filters assumes that the target birth intensity is known a priori. In situations where the targets can appear anywhere in the surveillance volume this is clearly inefficient, since the target birth intensity needs to cover the entire state space.

This paper presents a new extension of the PHD and CPHD filters, which distinguishes between the persistent and the newborn targets. This extension enables us to adaptively design the target birth intensity at each scan using the received measurements. Sequential Monte-Carlo implementations of the resulting PHD and CPHD filters are presented and their performance studied numerically. The proposed measurement driven birth intensity improves the estimation accuracy of both the number of targets and their spatial distribution.

Index Terms

Bayesian multi-object filtering, random finite set, probability hypothesis density (PHD), particle filter

I. INTRODUCTION

Mahler [1] recently proposed a systematic generalisation of the single-target recursive Bayes filter to the multi-target case. In this formulation, the targets can appear and disappear anywhere (within the state space of interest) and anytime (within the surveillance period), while target motion can be described by a nonlinear stochastic dynamic model. The sequentially received measurements are uncertain both due to the imperfections of the detection process (target detections could be missing and false detections can be present) and due to the stochastic nature of the

^a ISR Division, Defence Science and Technology Organisation, Bld 94, M2.30, 506 Lorimer Street, Melbourne, VIC 3207, Australia; Tel: (+61 3) 9626 8226; Fax: +61 3 9626 8341; email: branko.ristic@dsto.defence.gov.au

^b Joint Research Institute in Signal and Image Processing, Heriot-Watt University, Riccarton, Edinburgh, EH14 4AS, United Kingdom; Tel: +44 131 449 5111; email: D. E. Clark@hw.ac.uk

^c School of EECE, The University of Western Australia, 35 Stirling Hwy, Crawley, WA 6009, Australia; Tel: (+61 8) 6488 1767; fax: +61 8 6488 1065; email: ba-ngu.vo@uwa.edu.au

^d School of EECE, The University of Western Australia, 35 Stirling Hwy, Crawley, WA 6009, Australia; Tel: (+61 8) 6488 1767; fax: +61 8 6488 1065; email: ba-tuong.vo@uwa.edu.au

possibly nonlinear sensor model. The multi-target Bayes filter sequentially estimates the number of targets present and their individual states.

The Bayes filter propagates the posterior probability density function (pdf) through a two-step procedure: the prediction and update. In the multi-target case, the multi-target posterior pdf is formulated using the finite set statistics (FISST) [1], a set of practical mathematical tools from point process theory. The propagation of this multi-target posterior, however, is computationally very intensive due to the high dimensionality of the multi-target state space. If the state space of a single target is \mathcal{X} , the multi-target posterior pdf is defined on $\mathcal{F}(\mathcal{X})$, the space of finite subsets of \mathcal{X} . To overcome the high dimensionality of the multi-target Bayes filter, Mahler introduced the Probability Hypothesis Density (PHD) filter [2], which propagates the first moment of the multi-target posterior known as the intensity function or the PHD, defined on the single-target state-space \mathcal{X} . The resulting PHD filter subsequently became a very popular multi-target estimation method with applications in sonar [3], computer vision [4], [5], SLAM [6], traffic monitoring [7], biology [8], etc.

Since the intensity function is a very crude approximation of the multi-target pdf, Mahler subsequently introduced the Cardinalised PHD filter [9], which propagates both the intensity function and the cardinality distribution of the multi-target pdf. The resulting estimate of the number of targets is more stable than that of the PHD filter, as confirmed by numerical studies in [10]. The CPHD filter has been applied to GMTI tracking [11], tracking in the aerial videos [12], etc.

The standard formulations of both the PHD and CPHD filters assume that the target birth intensity is known a priori. Typically the birth intensity has the majority of its mass distributed over small specific areas of \mathcal{X} , which, for example in the air surveillance context, can be interpreted as the regions around airports [10], [13]. Note however that if a target appears in a region that is not covered by the predefined birth intensity, the PHD/CPHD filter will be completely blind to its existence. Making the target birth intensity diffuse so that it covers the entire state space of interest, typically results in a higher incidence of short-lived false tracks and longer confirmation times. The only way to overcome this drawback is to create at each processing step of the filter a massive number of potential (hypothesised) newborn targets covering the entire state-space, which is clearly inefficient. The described limitation affects both methods of PHD/CPHD filter implementation: the sequential Monte Carlo (SMC) method [14], [15] and the finite Gaussian mixtures (GM) [10], [13].

Starting from the standard equations of the PHD and the CPHD filter, in this paper we derive novel extensions which distinguish, in both the prediction and the update step, between the persistent and the newborn targets. This approach allows the PHD/CPHD filter to adapt the target birth intensity at each processing step using the received measurements. The resulting measurement driven birth intensity is very important in practice because it removes the need for the prior specification of birth intensities and eliminates the restriction on target appearance volumes within

\mathcal{X} . The paper presents an SMC implementation of proposed extensions of PHD and CPHD filters and demonstrates their improvement in performance by numerical examples.

Two remarks are in order here. First, we point out that the proposed measurement driven target birth intensity is complementary with the recent attempts to improve the efficiency of the SMC-PHD filter by pre-selecting particles for propagation (the so-called auxiliary particle PHD filter) presented in [15]. Second, the idea to use the measurements to adaptively build the target birth intensity has been proposed previously [16], [17]. Our paper, however, develops this initial idea much further.

II. BACKGROUND

Suppose that at time k there are n_k target states $\mathbf{x}_{k,1}, \dots, \mathbf{x}_{k,n_k}$, each taking values in a state space $\mathcal{X} \subseteq \mathbb{R}^{n_x}$, and m_k measurements (detections) $\mathbf{z}_{k,1}, \dots, \mathbf{z}_{k,m_k}$, each taking values in the observation space $\mathcal{Z} \subseteq \mathbb{R}^{n_z}$. A multi-target state and a multi-target observation are then represented by the finite sets:

$$\mathbf{X}_k = \{\mathbf{x}_{k,1}, \dots, \mathbf{x}_{k,n_k}\} \in \mathcal{F}(\mathcal{X}), \quad (1)$$

$$\mathbf{Z}_k = \{\mathbf{z}_{k,1}, \dots, \mathbf{z}_{k,m_k}\} \in \mathcal{F}(\mathcal{Z}), \quad (2)$$

respectively. Here $\mathcal{F}(\mathcal{X})$ and $\mathcal{F}(\mathcal{Z})$ are the finite subsets of \mathcal{X} and \mathcal{Z} , respectively. At each time step some targets may disappear (die), others may survive and transition into a new state, and new targets may appear. Due to the imperfections in the detector, some of the surviving and newborn targets may not be detected, whereas the observation set \mathbf{Z}_k may include false detections (or clutter). The evolution of the targets and the origin of measurements are unknown. Uncertainty in both multi-target state and multi-target measurement is naturally modelled by random finite sets.

The objective of the recursive multi-target Bayesian estimator [1] is to determine at each time step k the posterior probability density of multi-target state $f_{k|k}(\mathbf{X}_k|\mathbf{Z}_{1:k})$, where $\mathbf{Z}_{1:k} = (\mathbf{Z}_1, \dots, \mathbf{Z}_k)$ denotes the accumulated observation sets up to time k . The multi-target posterior is computed sequentially via the prediction and the update steps, see [1, ch.14].

Since $f_{k|k}(\mathbf{X}_k|\mathbf{Z}_{1:k})$ is defined over $\mathcal{F}(\mathcal{X})$, practical implementation of the multi-target Bayes filter is a difficult task and is usually limited to a small number of targets [18]–[20]. In order to overcome this limitation, Mahler proposed [2] to propagate only the first-order statistical moment of $f_{k|k}(\mathbf{X}_k|\mathbf{Z}_{1:k})$, referred to as the intensity function or the PHD, $D_{k|k}(\mathbf{x}|\mathbf{Z}_{1:k}) = \int \delta_{\mathbf{X}}(\mathbf{x})f_{k|k}(\mathbf{X}_k|\mathbf{Z}_{1:k})\delta\mathbf{X}$. In this definition $\delta_{\mathbf{X}}(\mathbf{x}) = \sum_{\mathbf{w} \in \mathbf{X}} \delta_{\mathbf{w}}(\mathbf{x})$. The integral of the PHD over \mathcal{X} ,

$$\int_{\mathcal{X}} D_{k|k}(\mathbf{x}|\mathbf{Z}_{1:k})d\mathbf{x} = \nu_{k|k} \in \mathbb{R}, \quad (3)$$

gives the (posterior) expected number of targets in the state space. The resulting PHD filter replaces the prediction and the update step of the multi-target Bayes filter with the much simpler expressions for the prediction and update

of the PHD (given in the next section).

Since the posterior PHD $D_{k|k}(\mathbf{x}|\mathbf{Z}_{1:k})$ is a very crude approximation of $f_{k|k}(\mathbf{X}|\mathbf{Z}_{1:k})$, Mahler subsequently proposed [9] to propagate the cardinality distribution $\rho(n) = \Pr(|\mathbf{X}| = n)$ given by:

$$\rho(n|\mathbf{Z}_{1:k}) = \frac{1}{n!} \int f_{k|k}(\{\mathbf{x}_1, \dots, \mathbf{x}_n\}|\mathbf{Z}_{1:k}) d\mathbf{x}_1 \dots \mathbf{x}_n, \quad (4)$$

jointly and alongside the PHD. The cardinality distribution satisfies the following condition: $\sum_{n=1}^{\infty} n\rho(n|\mathbf{Z}_{1:k}) = \int D_{k|k}(\mathbf{x}|\mathbf{Z}_{1:k}) d\mathbf{x} = \nu_{k|k}$. This is the basis of the CPHD filter.

III. EXTENSION OF THE PHD FILTER

The standard PHD filter equations are reviewed first, using the abbreviation $D_{k|k}(\mathbf{x}|\mathbf{Z}_{1:k}) \stackrel{\text{abbr}}{=} D_{k|k}(\mathbf{x})$. The prediction equation of the PHD filter is given by¹ [2]:

$$D_{k|k-1}(\mathbf{x}) = \gamma_{k|k-1}(\mathbf{x}) + \langle p_S D_{k-1|k-1}, \pi_{k|k-1}(\mathbf{x}|\cdot) \rangle \quad (5)$$

where

- $\gamma_{k|k-1}(\mathbf{x})$ is the PHD of target births between time k and $k+1$;
- $p_S(\mathbf{x}') \stackrel{\text{abbr}}{=} p_{S,k|k-1}(\mathbf{x}')$ is the probability that a target with state \mathbf{x}' at time $k-1$ will survive until time k ;
- $\pi_{k|k-1}(\mathbf{x}|\mathbf{x}')$ is the single-target transition density from time $k-1$ to k ;
- $\langle g, f \rangle = \int f(\mathbf{x}) g(\mathbf{x}) d\mathbf{x}$.

The first term on the RHS of (5) refers to the newborn targets, while the second represents the persistent targets.

Upon receiving the measurement set \mathbf{Z}_k at time k , the update step of the PHD filter is computed according to:

$$D_{k|k}(\mathbf{x}) = [1 - p_D(\mathbf{x})] D_{k|k-1}(\mathbf{x}) + \sum_{\mathbf{z} \in \mathbf{Z}_k} \frac{p_D(\mathbf{x}) g_k(\mathbf{z}|\mathbf{x}) D_{k|k-1}(\mathbf{x})}{\kappa_k(\mathbf{z}) + \langle p_D g_k(\mathbf{z}|\cdot), D_{k|k-1} \rangle} \quad (6)$$

where

- $p_D(\mathbf{x}) \stackrel{\text{abbr}}{=} p_{D,k}(\mathbf{x})$ is the probability that an observation will be collected at time k from a target with state \mathbf{x} ;
- $g_k(\mathbf{z}|\mathbf{x})$ is the single-target measurement likelihood at time k ;
- $\kappa_k(\mathbf{z})$ is the PHD of clutter at time k .

In the above formulation of the PHD filter, new targets are ‘‘born’’ in the prediction step (5). The intensity function of the newborn targets $\gamma_{k|k-1}(\mathbf{x})$ is independent of measurements, and in the general case, where the targets can appear anywhere in the state space, it has to cover the entire \mathcal{X} . This is significant for both the SMC and the GM implementation of the PHD filter, because the newborn target particles or Gaussian mixture components, need to cover the entire state-space with reasonable mass for the PHD filter to work properly. Clearly this is inefficient and wasteful.

¹We do not consider target spawning in this paper.

Instead we propose to design a newborn target intensity in the region of the state-space $\mathbf{x} \in \mathcal{X}$ for which the likelihood $g_k(\mathbf{z}|\mathbf{x})$ will have high values. We show that if the birth intensity is adapted in accordance with the measurements, *the PHD equations must be applied in a different form.*

Start from (5) and (6), where the state vector \mathbf{x} consists of the usual kinematic/feature component (position, velocity, amplitude, etc) which we denote by \mathbf{y} and a mark or a label β , which distinguishes a newborn target from the persistent target, i.e. $\mathbf{x} = (\mathbf{y}, \beta)$ where

$$\beta = \begin{cases} 0 & \text{for a persistent target} \\ 1 & \text{for a newborn target} \end{cases} \quad (7)$$

and $\mathbf{y} \in \mathcal{Y}$. The birth PHD is then:

$$\gamma_{k|k-1}(\mathbf{x}) = \gamma_{k|k-1}(\mathbf{y}, \beta) = \begin{cases} \gamma_{k|k-1}(\mathbf{y}), & \beta = 1 \\ 0, & \beta = 0. \end{cases} \quad (8)$$

Note a slight abuse of notation in using the same symbol $\gamma_{k|k-1}$ for both functions of \mathbf{x} and \mathbf{y} . Similar abuse will be used throughout this section, but the meaning should be clear from the context.

A newborn target becomes a persisting target at the next time, but a persisting target cannot become a newborn target. Thus the mark β can only change from 1 to 0 but not vice-versa. The transition model is then

$$\begin{aligned} \pi_{k|k-1}(\mathbf{x}|\mathbf{x}') &= \pi_{k|k-1}(\mathbf{y}, \beta|\mathbf{y}', \beta') \\ &= \pi_{k|k-1}(\mathbf{y}|\mathbf{y}')\pi_{k|k-1}(\beta|\beta') \end{aligned} \quad (9)$$

with

$$\pi_{k|k-1}(\beta|\beta') = \begin{cases} 0, & \beta = 1 \\ 1, & \beta = 0. \end{cases} \quad (10)$$

The probability of survival does not depend on β and hence

$$p_S(\mathbf{x}) = p_S(\mathbf{y}, \beta) = p_S(\mathbf{y}) \quad (11)$$

The PHD filter prediction equation (5) for the augmented state vector is given by:

$$D_{k|k-1}(\mathbf{y}, \beta) = \gamma_{k|k-1}(\mathbf{y}, \beta) + \sum_{\beta'=0}^1 \int D_{k-1|k-1}(\mathbf{y}', \beta') p_S(\mathbf{y}', \beta') \pi_{k|k-1}(\mathbf{y}, \beta|\mathbf{y}', \beta') d\mathbf{y}'. \quad (12)$$

Upon substitution of expressions (8)-(11) into (12) we obtain the new form of the PHD filter prediction:

$$D_{k|k-1}(\mathbf{y}, \beta) = \begin{cases} \gamma_{k|k-1}(\mathbf{y}), & \beta = 1 \\ \left\langle D_{k-1|k-1}(\cdot, 1) + D_{k-1|k-1}(\cdot, 0), p_S \pi_{k|k-1}(\mathbf{y}|\cdot) \right\rangle & \beta = 0 \end{cases} \quad (13)$$

Now we carry out similar manipulations for the update step. First, note that since the new targets are created from measurements, it follows that new targets are always detected (as they always generate measurements), so we can write:

$$p_D(\mathbf{x}) = p_D(\mathbf{y}, \beta) = \begin{cases} 1, & \beta = 1 \\ p_D(\mathbf{y}), & \beta = 0 \end{cases} \quad (14)$$

The measurement does not depend on β , hence

$$g_k(\mathbf{z}|\mathbf{x}) = g_k(\mathbf{z}|\mathbf{y}, \beta) = g_k(\mathbf{z}|\mathbf{y}). \quad (15)$$

The PHD update equation (6) for the augmented state vector is given by:

$$D_{k|k}(\mathbf{y}, \beta) = [1 - p_D(\mathbf{y}, \beta)]D_{k|k-1}(\mathbf{y}, \beta) + \sum_{\mathbf{z} \in \mathbf{Z}_k} \frac{p_D(\mathbf{y}, \beta)g_k(\mathbf{z}|\mathbf{y}, \beta)D_{k|k-1}(\mathbf{y}, \beta)}{\kappa_k(\mathbf{z}) + \sum_{\beta=0}^1 \langle p_D(\cdot, \beta)g_k(\mathbf{z}|\cdot, \beta), D_{k|k-1}(\cdot, \beta) \rangle} \quad (16)$$

Using (14) and (15), it follows that the update step for persisting targets ($\beta = 0$), is given by:

$$D_{k|k}(\mathbf{y}, 0) = [1 - p_D(\mathbf{y})]D_{k|k-1}(\mathbf{y}, 0) + \sum_{\mathbf{z} \in \mathbf{Z}_k} \frac{p_D(\mathbf{y})g_k(\mathbf{z}|\mathbf{y})D_{k|k-1}(\mathbf{y}, 0)}{\kappa_k(\mathbf{z}) + \langle g_k(\mathbf{z}|\cdot), \gamma_{k|k-1} \rangle + \langle p_D g_k(\mathbf{z}|\cdot), D_{k|k-1}(\cdot, 0) \rangle} \quad (17)$$

while the update step for newborn targets ($\beta = 1$) is given by:

$$D_{k|k}(\mathbf{y}, 1) = \sum_{\mathbf{z} \in \mathbf{Z}_k} \frac{g_k(\mathbf{z}|\mathbf{y}) \gamma_{k|k-1}(\mathbf{y})}{\kappa_k(\mathbf{z}) + \langle g_k(\mathbf{z}|\cdot), \gamma_{k|k-1} \rangle + \langle p_D g_k(\mathbf{z}|\cdot), D_{k|k-1}(\cdot, 0) \rangle} \quad (18)$$

Observe that both the prediction step and the update step are performed differently for newborn and persistent targets. The PHDs corresponding to the two types of targets are added together and predicted jointly in the prediction step, eq. (13), case $\beta = 0$.

IV. EXTENSION OF THE CARDINALISED PHD FILTER

Let $\rho_{k|k}(n|\mathbf{Z}_{1:n}) \stackrel{\text{abbr}}{=} \rho_{k|k}(n)$ denote the cardinality distribution at time k . Also, let $\rho_{\Gamma, k|k-1}(n) \stackrel{\text{abbr}}{=} \rho_{\Gamma}(n)$ denote the cardinality distribution of new targets at time k . The CPHD filter propagates both the cardinality distribution $\rho_{k|k}(n)$ and the PHD $D_{k|k}(\mathbf{x})$. We start again with the standard CPHD equations. In order to simplify our presentation assume that the probability of survival is constant, $p_S(\mathbf{x}) = p_S$. Then the predicted cardinality distribution can be written as a convolution [10]:

$$\rho_{k|k-1}(n) = \sum_{j=0}^n \rho_{S, k|k-1}(j) \rho_{\Gamma}(n-j) \quad (19)$$

where

$$\rho_{S, k|k-1}(j) = \sum_{\ell=j}^{\infty} \frac{\ell!}{j! (\ell-j)!} p_S^j (1-p_S)^{\ell-j} \rho_{k-1|k-1}(\ell) \quad (20)$$

is the predicted cardinality of survived targets. The predicted PHD is given by (5). Using the same reasoning as in the previous section, the prediction step of the CPHD filter, in terms of the newborn and persistent targets is given by (19) and (13).

The standard form of the CPHD filter update is given by:

$$\rho_{k|k}(n) = \frac{\Upsilon_k^0[D_{k|k-1}; \mathbf{Z}_k](n) \rho_{k|k-1}(n)}{\langle \Upsilon_k^0[D_{k|k-1}; \mathbf{Z}_k], \rho_{k|k-1} \rangle} \quad (21)$$

$$\begin{aligned} D_{k|k}(\mathbf{x}) &= (1 - p_D(\mathbf{x})) \frac{\langle \Upsilon_k^1[D_{k|k-1}; \mathbf{Z}_k], \rho_{k|k-1} \rangle}{\langle \Upsilon_k^0[D_{k|k-1}; \mathbf{Z}_k], \rho_{k|k-1} \rangle} D_{k|k-1}(\mathbf{x}) \\ &+ \sum_{\mathbf{z} \in \mathbf{Z}_k} \frac{\langle \Upsilon_k^1[D_{k|k-1}; \mathbf{Z}_k \setminus \{\mathbf{z}\}], \rho_{k|k-1} \rangle}{\langle \Upsilon_k^0[D_{k|k-1}; \mathbf{Z}_k], \rho_{k|k-1} \rangle} \frac{\langle 1, \kappa_k \rangle}{\kappa_k(\mathbf{z})} p_D(\mathbf{x}) g_k(\mathbf{z}|\mathbf{x}) D_{k|k-1}(\mathbf{x}) \end{aligned} \quad (22)$$

where

- the inner product between two real-valued sequences $\rho_1(n)$ and $\rho_2(n)$ is defined as $\langle \rho_1, \rho_2 \rangle = \sum_{n=0}^{\infty} \rho_1(n) \rho_2(n)$;
- the sequence $\Upsilon_k^u[D, \mathbf{Z}](n)$ is defined for $u \in \{0, 1\}$ as follows:

$$\Upsilon_k^u[D, \mathbf{Z}](n) = \sum_{j=0}^{\min(|\mathbf{Z}|, n)} (|\mathbf{Z}| - j)! \rho_{K,k}(|\mathbf{Z}| - j) P_{j+u}^n \frac{\langle 1 - p_D, D \rangle^{n-(j+u)}}{\langle 1, D \rangle^n} e_j(\Xi_k(D, \mathbf{Z})) \quad (23)$$

with

$$\Xi_k(D, \mathbf{Z}) = \left\{ \frac{\langle 1, \kappa_k \rangle}{\kappa_k(\mathbf{z})} \langle p_D D, g_k(\mathbf{z}|\cdot) \rangle : \mathbf{z} \in \mathbf{Z} \right\} \quad (24)$$

$$e_j(\mathbf{Z}) = \sum_{\mathbf{W} \subseteq \mathbf{Z}, |\mathbf{W}|=j} \left(\prod_{\zeta \in \mathbf{W}} \zeta \right) \quad (25)$$

$$P_\ell^n = \frac{n!}{(n - \ell)!} \quad (26)$$

Here $e_j(\mathbf{Z})$ is the elementary symmetric function (ESF) of order j for a finite set \mathbf{Z} [1, p.369], while $\rho_{K,k}(n)$ in (23) is the cardinality distribution of clutter at time k .

In order to express the CPHD filter update equations separately for the persistent and newborn targets, we will use the measurement model of (14) and (15). The update equation for cardinality distribution (21) still has the same form, while (22) can be now written as:

$$\begin{aligned} D_{k|k}(\mathbf{y}, \beta) &= (1 - p_D(\mathbf{y}, \beta)) \frac{\langle \Upsilon_k^1[D_{k|k-1}; \mathbf{Z}_k], \rho_{k|k-1} \rangle}{\langle \Upsilon_k^0[D_{k|k-1}; \mathbf{Z}_k], \rho_{k|k-1} \rangle} D_{k|k-1}(\mathbf{y}, \beta) \\ &+ \sum_{\mathbf{z} \in \mathbf{Z}_k} \frac{\langle \Upsilon_k^1[D_{k|k-1}; \mathbf{Z}_k \setminus \{\mathbf{z}\}], \rho_{k|k-1} \rangle}{\langle \Upsilon_k^0[D_{k|k-1}; \mathbf{Z}_k], \rho_{k|k-1} \rangle} \frac{\langle 1, \kappa_k \rangle}{\kappa_k(\mathbf{z})} p_D(\mathbf{y}, \beta) g_k(\mathbf{z}|\mathbf{y}, \beta) D_{k|k-1}(\mathbf{y}, \beta) \\ &= \begin{cases} \sum_{\mathbf{z} \in \mathbf{Z}_k} \frac{\langle 1, \kappa_k \rangle}{\kappa_k(\mathbf{z})} \frac{\langle \Upsilon_k^1[D_{k|k-1}; \mathbf{Z}_k \setminus \{\mathbf{z}\}], \rho_{k|k-1} \rangle}{\langle \Upsilon_k^0[D_{k|k-1}; \mathbf{Z}_k], \rho_{k|k-1} \rangle} g_k(\mathbf{z}|\mathbf{y}) \gamma_{k|k-1}(\mathbf{y}), & \beta = 1 \\ (1 - p_D(\mathbf{y})) \frac{\langle \Upsilon_k^1[D_{k|k-1}; \mathbf{Z}_k], \rho_{k|k-1} \rangle}{\langle \Upsilon_k^0[D_{k|k-1}; \mathbf{Z}_k], \rho_{k|k-1} \rangle} D_{k|k-1}(\mathbf{y}, 0) \\ + \sum_{\mathbf{z} \in \mathbf{Z}_k} \frac{\langle 1, \kappa_k \rangle}{\kappa_k(\mathbf{z})} \frac{\langle \Upsilon_k^1[D_{k|k-1}; \mathbf{Z}_k \setminus \{\mathbf{z}\}], \rho_{k|k-1} \rangle}{\langle \Upsilon_k^0[D_{k|k-1}; \mathbf{Z}_k], \rho_{k|k-1} \rangle} p_D(\mathbf{y}) g_k(\mathbf{z}|\mathbf{y}) D_{k|k-1}(\mathbf{y}, 0), & \beta = 0 \end{cases} \end{aligned} \quad (27)$$

with

$$\Upsilon_k^u[D_{k|k-1}, \mathbf{Z}](n) = \sum_{j=0}^{\min(|\mathbf{Z}|, n)} (|\mathbf{Z}| - j)! \rho_{K,k}(|\mathbf{Z}| - j) P_{j+u}^n \frac{\langle 1 - p_D(\cdot), D_{k|k-1}(\cdot, 0) \rangle^{n-(j+u)}}{\langle 1, D_{k|k-1}(\cdot, 1) + D_{k|k-1}(\cdot, 0) \rangle^n} e_j(\Xi_k(D_{k|k-1}, \mathbf{Z})) \quad (28)$$

and

$$\Xi_k(D_{k|k-1}, \mathbf{Z}) = \left\{ \frac{\langle 1, \kappa_k \rangle}{\kappa_k(\mathbf{z})} \langle D_{k|k-1}(\cdot, 1) + p_D(\cdot) D_{k|k-1}(\cdot, 0), g(\mathbf{z}|\cdot) \rangle : \mathbf{z} \in \mathbf{Z} \right\} \quad (29)$$

The above two equations are obtained by evaluation of the following expressions that appear in (23) and (24) :

$$\begin{aligned} \langle 1 - p_D, D \rangle &= \sum_{\beta=0}^1 \langle 1 - p_D(\cdot, \beta), D(\cdot, \beta) \rangle \\ &= \langle 1 - p_D(\cdot), D(\cdot, 0) \rangle \end{aligned} \quad (30)$$

$$\langle 1, D \rangle = \langle 1, D(\cdot, 0) + D(\cdot, 1) \rangle \quad (31)$$

$$\langle p_D D, g(\mathbf{z}|\cdot) \rangle = \langle D(\cdot, 1) + p_D(\cdot) D(\cdot, 0), g(\mathbf{z}|\cdot) \rangle \quad (32)$$

V. IMPLEMENTATION

We describe only the SMC implementation of the PHD and the CPHD filter with the target birth density driven by measurements. The pseudo-code of proposed SMC-PHD and SMC-CPHD filters is given in Algorithm 1 and 2, respectively. Initially, at the discrete-time index $k = 0$, the assumption is that $\rho_{0|0}(n) = 1$ if $n = 0$, and zero for $n = 1, 2, \dots, n_{\max}$ (n_{\max} represents the maximum anticipated number of targets), and $D_{0|0}(\mathbf{y}, 0) = D_{0|0}(\mathbf{y}, 1) = 0$. The random samples (particles) are used to approximate the intensity function. At time $k - 1$ we have:

$$D_{k-1|k-1}(\mathbf{y}, 0) \approx \sum_{n=1}^{N_{k-1}^p} w_{k-1,p}^{(n)} \delta_{\mathbf{y}_{k-1,p}^{(n)}}(\mathbf{y}) \quad (33)$$

$$D_{k-1|k-1}(\mathbf{y}, 1) \approx \sum_{n=1}^{N_{k-1}^b} w_{k-1,b}^{(n)} \delta_{\mathbf{y}_{k-1,b}^{(n)}}(\mathbf{y}) \quad (34)$$

where $\delta_{\mathbf{y}_0}(\mathbf{y})$ is the Dirac delta function [1, p.693], $\{(w_{k-1,p}^{(n)}, \mathbf{y}_{k-1,p}^{(n)})\}_{n=1}^{N_{k-1}^p}$ and $\{(w_{k-1,b}^{(n)}, \mathbf{y}_{k-1,b}^{(n)})\}_{n=1}^{N_{k-1}^b}$ are the weighted particle sets for persistent and newborn targets, respectively and N_{k-1}^p and N_{k-1}^b are the number of persistent target and newborn target particles, respectively. Before we apply the prediction step of the PHD or the CPHD filter, according to eq.(13), case $\beta = 0$), we need to sum-up the two intensity functions, $D_{k-1|k-1}(\mathbf{y}, 0)$ and $D_{k-1|k-1}(\mathbf{y}, 1)$. This summation is carried out by taking the union of the two particle sets, that is

$$\{(w_{k-1}^{(n)}, \mathbf{y}_{k-1}^{(n)})\}_{n=1}^{N_{k-1}} = \{(w_{k-1,p}^{(n)}, \mathbf{y}_{k-1,p}^{(n)})\}_{n=1}^{N_{k-1}^p} \cup \{(w_{k-1,b}^{(n)}, \mathbf{y}_{k-1,b}^{(n)})\}_{n=1}^{N_{k-1}^b} \quad (35)$$

is the random sample representation of $D_{k-1|k-1}(\mathbf{y}, 0) + D_{k-1|k-1}(\mathbf{y}, 1)$. The predicted intensity function $D_{k|k-1}(\mathbf{y}, 0)$ is approximated by the particle set:

$$D_{k|k-1}(\mathbf{y}, 0) \approx \sum_{n=1}^{N_{k-1}} w_{k|k-1,p}^{(n)} \delta_{\mathbf{y}_{k|k-1,p}^{(n)}}(\mathbf{y}), \quad (36)$$

where according to (13) for the $\beta = 0$ case:

$$\mathbf{y}_{k|k-1,p}^{(n)} \sim q_k(\cdot | \mathbf{y}_{k-1,p}^{(n)}, \mathbf{Z}_k) \quad (37)$$

$$w_{k|k-1,p}^{(n)} = \frac{p_S(\mathbf{y}_{k-1}^{(n)}) \pi_{k|k-1}(\mathbf{y}_{k|k-1,p}^{(n)} | \mathbf{y}_{k-1}^{(n)}) w_{k-1}^{(n)}}{q_k(\mathbf{y}_{k|k-1,p}^{(n)} | \mathbf{y}_{k-1,p}^{(n)}, \mathbf{Z}_k)} \quad (38)$$

with $q_k(\cdot|\mathbf{y}_{k-1}^{(n)}, \mathbf{Z}_k)$ being the importance density [21]. For simplicity of presentation we will sacrifice the efficiency of the SMC implementation and will adopt $q_k(\cdot|\mathbf{y}_{k-1}^{(n)}, \mathbf{Z}_k) = \pi_{k|k-1}(\cdot|\mathbf{y}_{k-1}^{(n)})$.

The $\beta = 1$ case in (13) is not implemented in a straightforward manner, because a massive number of particles would be required to approximate $D_{k|k-1}(\mathbf{y}, 1) = \gamma_{k|k-1}(\mathbf{y})$, of which the vast majority would be thrown away in the resampling step (to be carried out in the PHD/CPHD update). Instead, the idea is to use the current measurement set \mathbf{Z}_k to place the newborn particles in the region of the state space where the inner product $\langle g(\mathbf{z}|\cdot), \gamma_{k|k-1} \rangle$ will have non-zero values. Thus for each $\mathbf{z} \in \mathbf{Z}_k$, a set of M_b newborn particles $\mathbf{y}_{k|k-1,b}^{(n)}$ are generated in such a manner that \mathbf{z} can be considered as a random sample from the pdf $g_k(\cdot|\mathbf{y}_{k|k-1,b}^{(n)})$. This newborn target density, denoted by $b_k(\cdot|\mathbf{z})$ in line 14 of Algorithm 1, in practice can be approximated as follows. Suppose the target state vector \mathbf{y} consists of directly measured vector component \mathbf{p} and unmeasured vector component \mathbf{v} , that is $\mathbf{y} = [\mathbf{p}^\top \ \mathbf{v}^\top]^\top$, where \top denotes the matrix transpose. Let the measurement equation be: $\mathbf{z} = \mathbf{h}(\mathbf{p}) + \mathbf{w}$, where \mathbf{h} is an invertible function and $\mathbf{w} \sim \mathcal{N}(\mathbf{w}; \mathbf{0}, \mathbf{R})$ is zero-mean white Gaussian measurement noise with covariance \mathbf{R} . Then, particles $\mathbf{p}^{(n)}$, from the measured subspace of the target state space, can be drawn from $\mathcal{N}(\mathbf{y}; \mathbf{h}^{-1}(\mathbf{z}), \mathbf{H}_* \mathbf{R} \mathbf{H}_*^\top)$, where \mathbf{h}^{-1} is the inverse of \mathbf{h} and \mathbf{H}_* is the Jacobian of \mathbf{h}^{-1} . This, of course, is an approximation if \mathbf{h} is a nonlinear function [21]. The particles $\mathbf{v}^{(n)}$ from the unmeasured subspace need to be drawn from the prior.

The total number of newborn target particles generated in this way is $N_k^b = M_b \cdot |\mathbf{Z}_k|$. The weights of the new target particles are uniform, i.e.

$$w_{k|k-1,b}^{(n)} = \frac{\nu_{k|k-1}^b}{N_k^b} \quad (39)$$

where $\nu_{k|k-1}^b$ is the prior expected number of target births. The choice of this parameter of the PHD/CPHD filter is discussed later. In summary, the PHD filter birth intensity is modelled by an equally weighted mixture of birth densities $b_k(\cdot|\mathbf{z})$, for $\mathbf{z} \in \mathbf{Z}_k$, multiplied by the expected number of births $\nu_{k|k-1}^b$ (see lines 10 to 17 of Algorithm 1).

Consider next the update step of the PHD filter. Observe that upon the substitution of (36) into (17), $D_{k|k}(\mathbf{y}, 0)$ can be also written as the weighted sum of particles

$$D_{k|k}(\mathbf{y}, 0) \approx \sum_{n=1}^{N_{k-1}} w_{k|k,p}^{(n)} \delta_{\mathbf{y}_{k|k-1,p}^{(n)}}(\mathbf{y}), \quad (40)$$

where

$$w_{k|k,p}^{(n)} = (1 - p_D(\mathbf{y}_{k|k-1,p}^{(n)})) w_{k|k-1,p}^{(n)} + \sum_{\mathbf{z} \in \mathbf{Z}_k} \frac{p_D(\mathbf{y}_{k|k-1,p}^{(n)}) g_k(\mathbf{z}|\mathbf{y}_{k|k-1,p}^{(n)}) w_{k|k-1,p}^{(n)}}{\mathcal{L}(\mathbf{z})} \quad (41)$$

and

$$\mathcal{L}(\mathbf{z}) = \kappa_k(\mathbf{z}) + \sum_{n=1}^{N_k^b} w_{k|k-1,b}^{(n)} + \sum_{n=1}^{N_{k-1}} p_D(\mathbf{y}_{k|k-1,p}^{(n)}) g_k(\mathbf{z}|\mathbf{y}_{k|k-1,p}^{(n)}) w_{k|k-1,p}^{(n)} \quad (42)$$

Similarly it can be shown using (18) that $D_{k|k}(\mathbf{y}, 1)$ is approximated by the weighted particle set $\{(w_{k|k,b}^{(n)}, \mathbf{y}_{k|k-1,b}^{(n)})\}_{n=1}^{N_k^b}$ where:

$$w_{k|k,b}^{(n)} = \sum_{\mathbf{z} \in \mathbf{Z}_k} \frac{w_{k|k-1,b}^{(n)}}{\mathcal{L}(\mathbf{z})} \quad (43)$$

The particle set approximating the intensity function of persistent objects, $D_{k|k}(\mathbf{y}, 0)$, is next resampled N_k^p times in order to eliminate the samples with small weights and multiply the samples with large weights. The number of particles N_k^p is selected as:

$$N_k^p = \left\lceil M_p \cdot \sum_{n=1}^{N_{k-1}} w_{k|k,p}^{(n)} \right\rceil \quad (44)$$

where $\lceil \cdot \rceil$ denotes the nearest integer, M_p is the number of particles per persistent object (a parameter of the filter) and $\hat{\nu}_k^p = \sum_{n=1}^{N_{k-1}} w_{k|k,p}^{(n)}$ represents the posterior estimate of the number of persistent targets. After resampling the intensity function $D_{k|k}(\mathbf{y}, 0)$ is approximated by:

$$D_{k|k}(\mathbf{y}, 0) \approx \sum_{n=1}^{N_k^p} w_{k,p}^{(n)} \delta_{\mathbf{y}_{k,p}^{(n)}}(\mathbf{y}) \quad (45)$$

where $w_{k,p}^{(n)} = \hat{\nu}_k^p / N_k^p$. The PHD filter reports at time k only the intensity function of persistent targets $D_{k|k}(\mathbf{y}, 0)$.

The particle set approximating the intensity function of newborn objects, $D_{k|k}(\mathbf{y}, 1)$, can be also resampled, although this is not essential (line 23 in Alg. 1). The value of $\nu_{k|k-1}^b$ in (39) has to be chosen in such a manner that the sum $\hat{\nu}_k^b = \sum_{n=1}^{N_{k-1}^b} w_{k|k,b}^{(n)}$ corresponds to the expected number of newborn objects at time k .

In the implementation of the SMC-CPHD filter it is necessary to propagate (predict and update) the cardinality distribution (see Algorithm 2 for details). The prediction step of the SMC-CPHD filter is straightforward. The update step first requires to compute three inner products in (29) and (28). Using the particle representation of the intensity functions $D_{k|k-1}(\mathbf{y}, 0)$ and $D_{k|k-1}(\mathbf{y}, 1)$ this can be done as follows:

$$\langle 1 - p_D(\cdot), D_{k|k-1}(\cdot, 0) \rangle \approx \sum_{n=1}^{N_{k-1}} (1 - p_D(\mathbf{y}_{k|k-1,p}^{(n)})) w_{k|k-1,p}^{(n)} \quad (46)$$

$$\langle 1, D_{k|k-1}(\cdot, 1) + D_{k|k-1}(\cdot, 0) \rangle \approx \sum_{n=1}^{N_{k-1}} w_{k|k-1,p}^{(n)} + \sum_{n=1}^{N_k^b} w_{k|k-1,b}^{(n)} \quad (47)$$

$$\langle D_{k|k-1}(\cdot, 1) + p_D(\cdot) D_{k|k-1}(\cdot, 0), g(\mathbf{z}|\cdot) \rangle \approx \sum_{n=1}^{N_{k-1}} p_D(\mathbf{y}_{k|k-1,p}^{(n)}) g_k(\mathbf{z}|\mathbf{y}_{k|k-1,p}^{(n)}) w_{k|k-1,p}^{(n)} + \sum_{n=1}^{N_k^b} w_{k|k-1,b}^{(n)} \quad (48)$$

Computation of ESFs $e_j(\Xi_k(D_{k|k-1}, \mathbf{Z}))$, required in (28), is described in [10].

Algorithm 1 Processing steps of the SMC-PHD filter at time k

-
- 1: **Input:**
 - 2: a) Particle representation of $D_{k-1|k-1}(\mathbf{y}, 0)$: $\{(w_{k-1,p}^{(n)}, \mathbf{y}_{k-1,p}^{(n)})\}_{n=1}^{N_{k-1}^p}$ ▷ Eq. (33)
 - 3: b) Particle representation of $D_{k-1|k-1}(\mathbf{y}, 1)$: $\{(w_{k-1,b}^{(n)}, \mathbf{y}_{k-1,b}^{(n)})\}_{n=1}^{N_{k-1}^b}$ ▷ Eq. (34)
 - 4: c) Measurement set at k : $\mathbf{Z}_k = \{\mathbf{z}_{k,1}, \dots, \mathbf{z}_{k,m_k}\}$; Note: $m_k = |\mathbf{Z}_k|$
 - 5: $\{(w_{k-1}^{(n)}, \mathbf{y}_{k-1}^{(n)})\}_{n=1}^{N_{k-1}} = \{(w_{k-1,p}^{(n)}, \mathbf{y}_{k-1,p}^{(n)})\}_{n=1}^{N_{k-1}^p} \cup \{(w_{k-1,b}^{(n)}, \mathbf{y}_{k-1,b}^{(n)})\}_{n=1}^{N_{k-1}^b}$ ▷ Union of input particle sets, Eq. (35)
 - 6: **for** $n = 1, \dots, N_{k-1}$ **do** ▷ Random sample approximation of $D_{k|k-1}(\mathbf{y}, 0)$
 - 7: Draw $\mathbf{y}_{k|k-1,p}^{(n)} \sim \pi_{k|k-1}(\cdot | \mathbf{y}_{k-1}^{(n)})$ ▷ Eq. (37)
 - 8: Compute weight $w_{k|k-1,p}^{(n)} = p_S(\mathbf{y}_{k-1}^{(n)})w_{k-1}^{(n)}$ ▷ Eq. (38)
 - 9: **end for**
 - 10: $N_k^b = M_b \cdot m_k$ ▷ Parameter M_b : the number of particles per newborn target
 - 11: **for** $j = 1, \dots, m_k$ **do** ▷ Random sample approximation of $D_{k|k-1}(\mathbf{y}, 1) = \gamma_{k|k-1}(\mathbf{y})$
 - 12: **for** $\ell = 1, \dots, M_b$ **do**
 - 13: $n = \ell + (j-1)M_b$
 - 14: Draw $\mathbf{y}_{k|k-1,b}^{(n)} \sim b_k(\cdot | \mathbf{z}_{k,j})$ ▷ b_k depends on $g_k(\mathbf{z} | \mathbf{y})$ and prior knowledge
 - 15: Compute weight $w_{k|k-1,b}^{(n)} = \nu_{k|k-1}^b / N_k^b$ ▷ Parameter $\nu_{k|k-1}^b$
 - 16: **end for**
 - 17: **end for**
 - 18: Compute $w_{k|k,p}^{(n)}$, $n = 1, \dots, N_{k-1}$ using Eq.(41)
 - 19: Compute $w_{k|k,b}^{(n)}$, $n = 1, \dots, N_k^b$ using Eq.(43)
 - 20: Compute $\hat{\nu}_k^p = \sum_{n=1}^{N_{k-1}} w_{k|k,p}^{(n)}$; $\hat{\nu}_k^b = \sum_{n=1}^{N_k^b} w_{k|k,b}^{(n)}$ ▷ Estimated number of persistent and newborn objects
 - 21: $N_k^p = [M_p \hat{\nu}_k^p]$ ▷ Eq. (44), Parameter M_p : the number of particles per persistent target
 - 22: Resample N_k^p times from $\{(w_{k|k,p}^{(n)} / \hat{\nu}_k^p, \mathbf{y}_{k|k-1,p}^{(n)})\}_{n=1}^{N_{k-1}}$ to obtain $\{(w_{k,p}^{(n)}, \mathbf{y}_{k,p}^{(n)})\}_{n=1}^{N_k^p}$, with $w_{k,p}^{(n)} = \hat{\nu}_k^p / N_k^p$.
 - 23: Resample N_k^b times from $\{(w_{k|k,b}^{(n)} / \hat{\nu}_k^b, \mathbf{y}_{k|k-1,b}^{(n)})\}_{n=1}^{N_k^b}$ to obtain $\{(w_{k,b}^{(n)}, \mathbf{y}_{k,b}^{(n)})\}_{n=1}^{N_k^b}$, with $w_{k,b}^{(n)} = \hat{\nu}_k^b / N_k^b$.
 - 24: **Report:** particle representation of $D_{k|k}(\mathbf{y}, 0)$: $\{(w_{k,p}^{(n)}, \mathbf{y}_{k,p}^{(n)})\}_{n=1}^{N_k^p}$; cardinality estimate $\hat{\nu}_k^p$.
-

VI. NUMERICAL RESULTS

A. Simulation setup

The performance of the described PHD and CPHD filters with target birth density driven by measurements is demonstrated using a scenario with up to ten targets. The top down view of target trajectories is shown in Fig.1. The starting point of each trajectory is indicated by sign \circ . The state vector of an individual target consists of a position and velocity in x and y coordinates, that is $\mathbf{y} = [x, \dot{x}, y, \dot{y}]^\top$. The transitional density is $\pi_{k|k-1}(\mathbf{y} | \mathbf{y}') = \mathcal{N}(\mathbf{y}; \mathbf{F}\mathbf{y}', \mathbf{Q})$, where $\mathcal{N}(\cdot; \mathbf{m}, \mathbf{P})$ denotes a Gaussian pdf with mean \mathbf{m} and covariance \mathbf{P} , matrix $\mathbf{F} = \mathbf{I}_2 \otimes \begin{pmatrix} 1 & T \\ 0 & 1 \end{pmatrix}$, T is the sampling interval, \otimes is the Kroneker product, \mathbf{I}_m is the $m \times m$ identity matrix, and $\mathbf{Q} = \mathbf{I}_2 \otimes q \begin{pmatrix} T^3/3 & T^2/2 \\ T^2/2 & T \end{pmatrix}$, with q being process noise intensity. We used in simulations $T = 1s$, $q = 0.30$. The probability of survival was set to $p_S = 0.98$.

The measurements of target range and bearing are collected by a sensor placed at $(x_s, y_s) = (-100m, -100m)$.

Algorithm 2 Processing steps of the SMC-CPHD filter at time k

-
- 1: **Input:**
 - 2: a) Cardinality distribution $\rho_{k-1|k-1}(n)$
 - 3: b) particle representation of $D_{k-1|k-1}(\mathbf{y}, 0)$: $\{(w_{k-1,p}^{(n)}, \mathbf{y}_{k-1,p}^{(n)})\}_{n=1}^{N_{k-1}^p}$
 - 4: c) Particle representation of $D_{k-1|k-1}(\mathbf{y}, 1)$: $\{(w_{k-1,b}^{(n)}, \mathbf{y}_{k-1,b}^{(n)})\}_{n=1}^{N_{k-1}^b}$
 - 5: c) Measurement set at k : $\mathbf{Z}_k = \{\mathbf{z}_{k,1}, \dots, \mathbf{z}_{k,m_k}\}$;
 - 6: Prediction of cardinality distribution, Eq. (19);
 - 7: Union of input particle sets, Eq. (35)
 - 8: Prediction of persistent target particles (lines 6-9 in Alg.1)
 - 9: Creation of newborn target particles (lines 10-17 in Alg.1)
 - 10: Computation of elements in $\Xi_k(D_{k|k-1}, \mathbf{Z}_k)$, Eq.(29)
 - 11: Computation of ESFs, $e_j(\Xi_k(D_{k|k-1}, \mathbf{Z}_k))$
 - 12: Computation of $\Upsilon_k^u[D_{k|k-1}, \mathbf{Z}_k](n)$, Eq. (28), for $u = 1, 0$
 - 13: **for** every $\mathbf{z} \in \mathbf{Z}_k$ **do**
 - 14: Compute $\Xi_k(D_{k|k-1}, \mathbf{Z}_k \setminus \{\mathbf{z}\})$, $e_j(\Xi_k(D_{k|k-1}, \mathbf{Z}_k \setminus \{\mathbf{z}\}))$, $\Upsilon_k^1[D_{k|k-1}, \mathbf{Z}_k \setminus \{\mathbf{z}\}](n)$
 - 15: **end for**
 - 16: Update cardinality distribution, Eq.(21)
 - 17: Update weights $w_{k|k,p}^{(n)}$, $n = 1, \dots, N_{k-1}$ using Eq.(27), case $\beta = 0$
 - 18: Update weights $w_{k|k,b}^{(n)}$, $n = 1, \dots, N_k^b$ using Eq.(27), case $\beta = 1$
 - 19: Compute $\hat{\nu}_k^p = \sum_{n=1}^{N_{k-1}} w_{k|k,p}^{(n)}$; $\hat{\nu}_k^b = \sum_{n=1}^{N_k^b} w_{k|k,b}^{(n)}$ ▷ Estimated number of persistent and newborn objects
 - 20: $N_k^p = [M_p \hat{\nu}_k^p]$
 - 21: Resample N_k^p times from $\{(w_{k|k,p}^{(n)}/\hat{\nu}_k^p, \mathbf{y}_{k|k-1,p}^{(n)})\}_{n=1}^{N_{k-1}}$ to obtain $\{(w_{k,p}^{(n)}, \mathbf{y}_{k,p}^{(n)})\}_{n=1}^{N_k^p}$, with $w_{k,p}^{(n)} = \hat{\nu}_k^p/N_k^p$.
 - 22: Resample N_k^b times from $\{(w_{k|k,b}^{(n)}/\hat{\nu}_k^b, \mathbf{y}_{k|k-1,b}^{(n)})\}_{n=1}^{N_k^b}$ to obtain $\{(w_{k,b}^{(n)}, \mathbf{y}_{k,b}^{(n)})\}_{n=1}^{N_k^b}$, with $w_{k,b}^{(n)} = \hat{\nu}_k^b/N_k^b$.
 - 23: **Report:**
 - 24: a) Estimated cardinality distribution $\rho_{k|k}(n)$;
 - 25: b) particle representation of $D_{k|k}(\mathbf{y}, 0)$: $\{(w_{k,p}^{(n)}, \mathbf{y}_{k,p}^{(n)})\}_{n=1}^{N_k^p}$
-

The measurement likelihood is then $g_k(\mathbf{z}|\mathbf{y}) = \mathcal{N}(\mathbf{z}; \mathbf{h}(\mathbf{y}), \mathbf{R})$, where

$$\mathbf{h}(\mathbf{y}) = \begin{pmatrix} \sqrt{(x - x_s)^2 + (y - y_s)^2} \\ \arctan \frac{x - x_s}{y - y_s} \end{pmatrix}. \quad (49)$$

and $\mathbf{R} = \text{diag}(\sigma_r^2, \sigma_b^2)$. The range measurements are very precise ($\sigma_r = 0.1\text{m}$) while the bearing measurements are fairly inaccurate (i.e. $\sigma_b = 2$ degrees). Consequently the measurement uncertainty regions are arcs with $\pm 3\sigma$ angular span of 12 degrees. Kalman type filters, which assume the measurement uncertainty regions to be ellipsoids, would be inappropriate in this case, thus justifying the need for an SMC implementation. The clutter is uniformly distributed along the range (from 0 to 1300 m) and bearing ($\pm\pi/4$ rad with respect to the sensor pointing direction). The number of clutter points per scan is Poisson distributed with the mean value of $\lambda = 10$. The probability of detection is $p_D = 0.95$. For every measurement $\mathbf{z} \in \mathbf{Z}_k$, the newborn target particle positions are:

$$\begin{aligned} x_k^{(n)} &= x_s + (\mathbf{z}[1] + \sigma_r v_1^{(n)}) \sin(\mathbf{z}[2] + \sigma_b v_2^{(n)}) \\ y_k^{(n)} &= y_s + (\mathbf{z}[1] + \sigma_r v_1^{(n)}) \cos(\mathbf{z}[2] + \sigma_b v_2^{(n)}) \end{aligned}$$

where $n = 1, \dots, N_k^b$, $\mathbf{z}[1]$ and $\mathbf{z}[2]$ are the measured range and bearing and $v_1^{(n)}, v_2^{(n)} \sim \mathcal{N}(\cdot; 0, 1)$. The particle velocities are generated as $\dot{x}_k^{(n)}, \dot{y}_k^{(n)} \sim \mathcal{N}(\cdot; 0, \sigma_V^2)$, where $\sigma_V = 5\text{m/s}$.

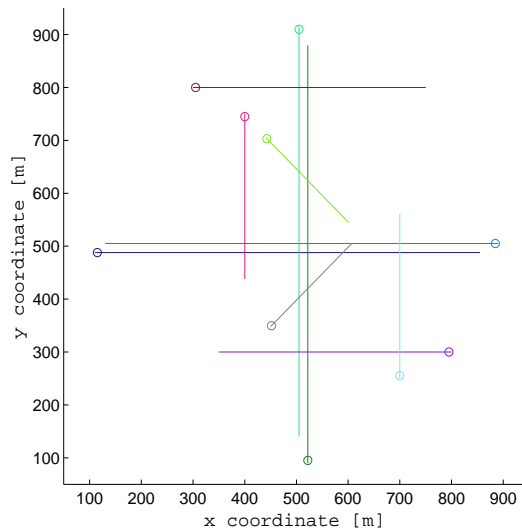


Fig. 1. Target trajectories shown in $x - y$ plane. Starting points denoted by \circ .

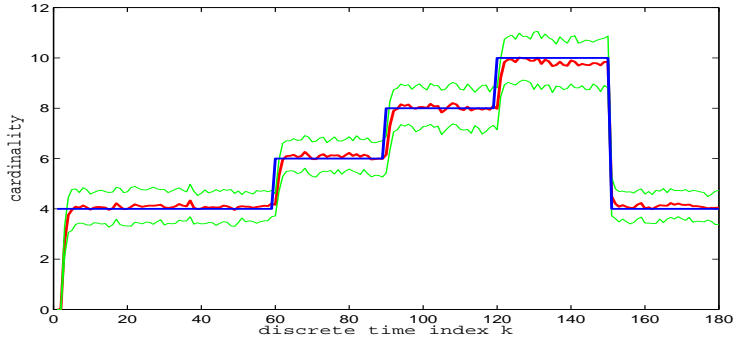
In both PHD and CPHD filters $M_b = M_p = 3000$ particles. The parameter $\nu_{k|k-1}^b = 0.0001$ is selected so that the average number of newborn targets per scan is $\hat{\nu}_k^b \approx 0.25$. The cardinality distribution of newborn targets is assumed Poisson. Parameter n_{\max} in the CPHD filter is set to 30.

B. Error performance analysis

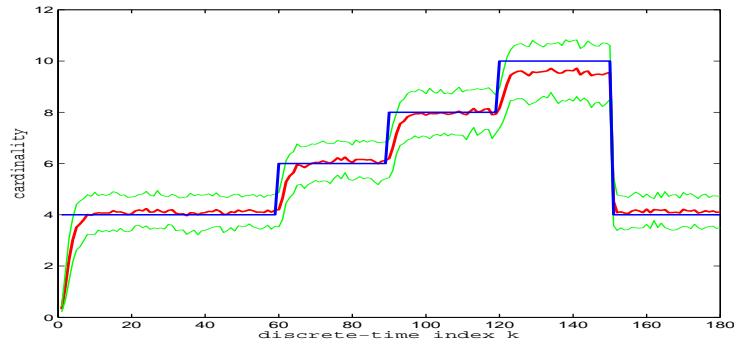
The performance of the PHD/CPHD filters is measured by two methods. The first method compares the true and the estimated cardinality value over time, that is n_k and $\hat{\nu}_k^p$, respectively. The second method measures the concentration of particles around the true target positions. In comparisons, we consider three contesting filters: (a) PHDF-M: the described PHD filter with the measurement driven birth intensity; (b) PHDF-U: the PHD filter which places M_b newborn target particles uniformly across range (from 0 to 1300 m) and bearing ($\pm\pi/4$ rad with respect to the sensor pointing direction); the velocities are generated as $\dot{x}_k^{(n)}, \dot{y}_k^{(n)} \sim \mathcal{N}(\cdot; 0, \sigma_V^2)$, with $\sigma_V = 5\text{m/s}$; (c) CPHDF-M: the described CPHD filter with the measurement driven birth intensity. In order to make the comparison fair, for all three filters, an equal value of the average number of newborn targets per scan is adopted ($\hat{\nu}_k^b \approx 0.25$).

a) Cardinality estimation.: Fig.2 shows the true and estimated posterior cardinality value (the number of targets) over time obtained using the three contesting filters. The estimated cardinality curves were obtained by averaging over 100 Monte Carlo runs. The colour coding is as follows: the true number of targets is plotted by a solid blue line, the mean estimated number of targets by a solid red line and the plus/minus one standard deviation of the estimated number of targets by two green lines. Observe that the two PHD filters (PHDF-M and PHDF-U) perform similarly with respect to the cardinality estimation. There are, however, two noticeable differences: (a) the PHDF-U underestimates cardinality in the presence of 10 targets and (b) PHDF-M responds more quickly to the changes in target number. Regarding the comparison of the PHDF-M versus the CPHDF-M, the results are in a good

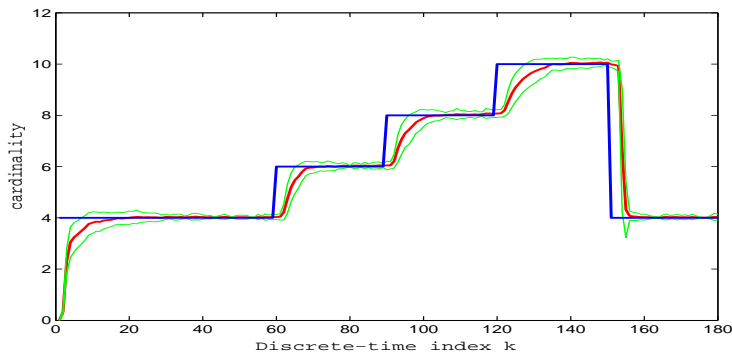
agreement with those reported in [10]: both filters produce unbiased cardinality estimates in the steady-state, but the PHD cardinality estimate is more responsive to the changes in cardinality. The CPHDF-M cardinality estimate, on the other hand, has a much smaller variance.



(a)



(b)



(c)

Fig. 2. True versus estimated cardinality over time: (a) PHDF-M; (b) PHDF-U; (c) CPHDF-M. Colour coding: blue line is true; red line is estimated (averaged); green lines are ± 1 standard deviation

b) Spatial distribution estimation.: Next we want to measure the concentration of particles around the true target locations in the state-space. For this purpose we need to introduce the posterior spatial distribution of persistent

targets, $s_{k|k}(\mathbf{y}, \beta = 0 | \mathbf{Z}_{1:k}) \stackrel{\text{abbr}}{=} s_{k|k}(\mathbf{y})$ defined as:

$$s_{k|k}(\mathbf{y}) = \frac{D_{k|k}(\mathbf{y}, 0)}{\int D_{k|k}(\mathbf{y}, 0) d\mathbf{y}} \quad (50)$$

The SMC estimate of the PHD of persisting targets, $D_{k|k}(\mathbf{y}, 0)$, as reported by a PHD/CPHD filter, was given in (45). The SMC estimate of $s_{k|k}(\mathbf{y})$ of (50) is then:

$$\hat{s}_{k|k}(\mathbf{y}) = \sum_{n=1}^{N_k^p} \tilde{w}_{k,p}^{(n)} \cdot \delta_{\mathbf{y}_{k,p}^{(n)}}(\mathbf{y}) \quad (51)$$

where

$$\tilde{w}_{k,p}^{(n)} = \frac{w_{k,p}^{(n)}}{\sum_{n=1}^{N_k^p} w_{k,p}^{(n)}} \quad (52)$$

are normalised weights (as opposed to PHD weights $w_{k,p}^{(n)}$ introduced in (45)).

The spatial distribution of the ‘‘ground truth’’ is defined as

$$s_k(\mathbf{y}) = \frac{1}{n_k} \sum_{i=1}^{n_k} \delta_{\mathbf{y}_{k,i}}(\mathbf{y}) \quad (53)$$

where $\{\mathbf{y}_{k,1}, \dots, \mathbf{y}_{k,n_k}\}$ is the true multi-target state at time k .

The similarity between the ground truth $s_k(\mathbf{y})$ of (53) and the PHD/CPHD filter estimate $\hat{s}_{k|k}(\mathbf{y})$ of (51), will be measured using the Bhattacharyya distance [22]:

$$B(s_k, \hat{s}_{k|k}) = -\ln \int \sqrt{s_k(\mathbf{y})} \sqrt{\hat{s}_{k|k}(\mathbf{y})} d\mathbf{y} \quad (54)$$

Clearly $B(s, u) \geq 0$. In addition, identity and symmetry properties are satisfied, i.e. $B(s, s) = 0$ and $B(s, u) = B(u, s)$, respectively. The triangle inequality is not guaranteed.

In order to compute the integral in (54), it is first necessary to select a common set of support points for both s_k and $\hat{s}_{k|k}$. Let the common set of support points be the true multi-target state $\{\mathbf{y}_{k,1}, \dots, \mathbf{y}_{k,n_k}\}$. Then we need to determine the values of $\hat{s}_{k|k}(\mathbf{y})$ at points $\mathbf{y}_{k,i}$, for $i = 1, \dots, n_k$. Using kernel density estimation [23], we have:

$$\hat{s}_{k|k}(\mathbf{y}_{k,i}) = Q_{k,i} \approx \frac{1}{W^{n_x}} \sum_{n=1}^{N_k^p} \tilde{w}_{k,p}^{(n)} \cdot \phi\left(\frac{\mathbf{y}_{k,i} - \mathbf{y}_{k,p}^{(n)}}{W}\right) \quad (55)$$

where W is the kernel width, $n_x = 4$, and ϕ is the kernel function which we adopt to be Gaussian (the expression for optimal W is given in [23]).

Following the arguments presented in [24, Appendix], the substitution of $s_k(\mathbf{y})$ of (53) and

$$\hat{s}_{k|k}(\mathbf{y}) \approx \sum_{i=1}^{n_k} Q_{k,i} \delta_{\mathbf{y}_{k,i}}(\mathbf{y})$$

into (54) leads to

$$B(s_k, \hat{s}_{k|k}) \approx -\ln \left(\sum_{i=1}^{n_k} \sqrt{\frac{Q_{k,i}}{n_k}} \right) \quad (56)$$

This distance measure will be used to evaluate the error performance of particle PHD/CPHD spatial distribution estimate.

Fig.3 displays the Bhattacharyya distance (56) averaged over 100 Monte Carlo runs, for all three contesting filters: PHDF-M, PHDF-U and CPHDF-M. Observe first that the proposed PHD/CPHD filters with measurement driven birth intensity (PHDF-M and CPHDF-M) result in vastly more accurate approximations of the true spatial density than the PHDF-U. This indicates that both the PHDF-M and the CPHDF-M cluster their particles around the true state better. This result confirms the importance of the measurement driven approach to birth intensity in PHD/CPHD filters.

With regards to the comparison between the PHDF-M and CPHDF-M, note that in the steady-state the Bhattacharyya distance for the CPHD filter is slightly lower. This is a significant observation since it shows that the CPHD filter, in the steady state, not only provides more stable cardinality estimates, but also achieves a more accurate spatial density estimation.

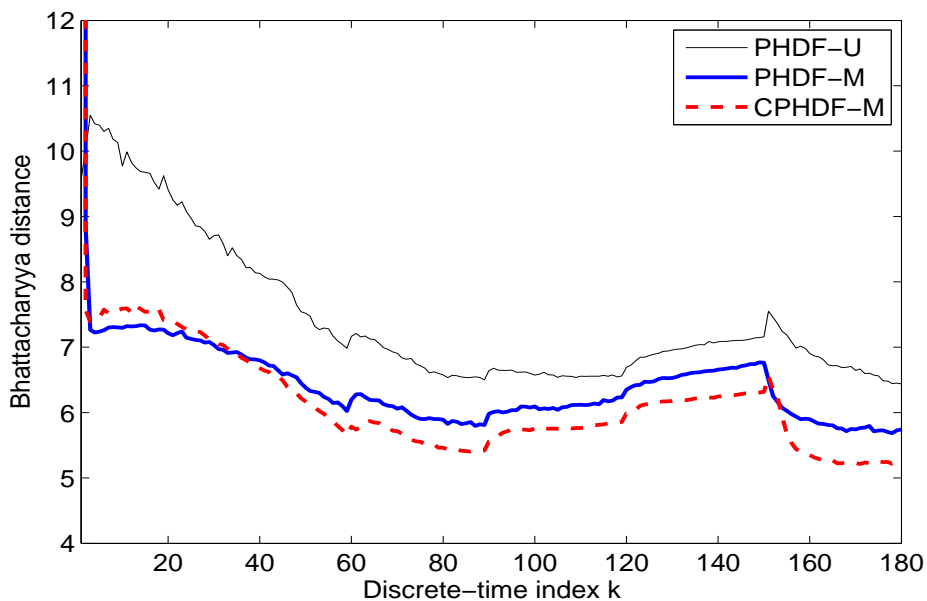


Fig. 3. Average Bhattacharyya distance between the true and estimated spatial density over time: PHDF-M (blue thick line); PHDF-U (black thin line); CPHDF-M filter (red dashed line)

VII. CONCLUSIONS

The paper presented an extension of the PHD and the Cardinalised PHD filters, distinguishing between the newborn and persistent targets. Using this approach it was possible to design a PHD/CPHD filter with measurement driven target birth intensity, thus relaxing the previously imposed limitation that target appearance (birth) intensity is a priori known. Sequential Monte Carlo implementations of the resulting PHD and CPHD filters were studied

by numerical simulations. It has been observed that the measurement driven target birth intensity concept results in the higher estimation accuracy of the true intensity function. With regards to the comparison between the proposed PHD and CPHD filters, their performance is found to be in agreement with the previously reported results: the PHD filter is more responsive to the changes in cardinality, but its cardinality estimates have a higher variance; the CPHD filter is also found to be slightly more accurate in estimating the spatial distribution in the steady state.

REFERENCES

- [1] R. Mahler, *Statistical Multisource Multitarget Information Fusion*. Artech House, 2007.
- [2] R. P. S. Mahler, "Multi-target Bayes filtering via first-order multi-target moments," *IEEE Trans. Aerospace & Electronic Systems*, vol. 39, no. 4, pp. 1152–1178, 2003.
- [3] D. Clark, I. T. Ruiz, Y. Petillot, and J. Bell, "Particle PHD filter multiple target tracking in sonar image," *IEEE Trans. Aerospace & Electronic Systems*, vol. 43, no. 1, pp. 409–416, 2007.
- [4] E. Maggio, M. Taj, and A. Cavallaro, "Efficient multitarget visual tracking using random finite sets," *IEEE Trans. Circuits & Systems for Video Technology*, vol. 18, no. 8, pp. 1016–1027, 2008.
- [5] N. T. Pham, W. Huang, and S. H. Ong, "Tracking multiple objects using Probability Hypothesis Density filter and color measurements," in *Proc. IEEE Int. Conf. Multimedia and Expo*, July 2007, pp. 1511 – 1514.
- [6] J. Mullane, B.-N. Vo, and M. D. Adams, "Rao-Blackwellised PHD SLAM," in *Proc. IEEE Int. Conf. Robotics and Automation*, Alaska, USA, May 2010.
- [7] G. Battistelli, L. Chisci, S. Morrocchi, F. Papi, A. Benavoli, A. D. Lallo, A. Farina, and A. Graziano, "Traffic intensity estimation via PHD filtering," in *Proc. 5th European Radar Conf.*, Amsterdam, The Netherlands, Oct. 2008, pp. 340–343.
- [8] R. R. Juang, A. Levchenko, and P. Burlina, "Tracking cell motion using GM-PHD," in *Int. Symp. Biomedical Imaging*, June/July 2009, pp. 1154–1157.
- [9] R. P. S. Mahler, "PHD filters of higher order in target number," *IEEE Trans. Aerospace & Electronic Systems*, vol. 43, no. 4, pp. 1523–1543, 2007.
- [10] B.-T. Vo, B.-N. Vo, and A. Cantoni, "Analytic implementations of the cardinalized probability hypothesis density filter," *IEEE Trans. Signal Processing*, vol. 55, no. 7, pp. 3553–3567, 2007.
- [11] M. Ulmke, O. Erdinc, and P. Willett, "GMTI tracking via the Gaussian mixture cardinalized probability hypothesis density filter," *IEEE Trans. Aerospace & Electronic Systems*, vol. 46, no. 4, pp. 1821–1833, 2010.
- [12] E. Pollard, A. Plyer, B. Pannetier, F. Champagnat, and G. L. Besnerais, "GM-PHD filters for multi-object tracking in uncalibrated aerial videos," *Proc. 12th Int. Conf. Information Fusion*, pp. 1171–1178, July 2009.
- [13] B.-N. Vo and W.-K. Ma, "The Gaussian mixture probability hypothesis density filter," *IEEE Trans. Signal Processing*, vol. 54, no. 11, pp. 4091–4104, Nov. 2006.
- [14] B. N. Vo, S. Singh, and A. Doucet, "Sequential Monte Carlo methods for multi-target filtering with random finite sets," *IEEE Trans. Aerospace & Electronic Systems*, vol. 41, no. 4, pp. 1224–1245, Oct. 2005.
- [15] N. P. Whiteley, S. S. Singh, and S. J. Godsill, "Auxiliary particle implementation of the probability hypothesis density filter," *IEEE Trans. on Aerospace & Electronic Systems*, 2009, to appear.
- [16] M. Tobias and A. Lanterman, "Techniques for birth-particle placement in the probability hypothesis density particle filter applied to passive radar," *IET Radar Sonar Navig.*, vol. 2, no. 5, pp. 351–365, 2008.
- [17] R. L. Streit and L. D. Stone, "Bayes derivation of multitarget intensity filters," in *Proc. 11th Intl. Conf. Information Fusion*. Cologne, Germany: ISIF, July 2008.
- [18] H. Sidenbladh and S. L. Wirkander, "Tracking random sets of vehicles in terrain," in *Proc. 2nd IEEE Workshop on Multi-Object Tracking*, Madison, WI, USA, June 2003.

- [19] M. Vihola, "Rao-Blackwellised particle filtering in random set multitarget tracking," *IEEE Trans. Aerospace & Electronic Systems*, vol. 43, no. 2, pp. 689–705, 2007.
- [20] B. Ristic and B.-N. Vo, "Sensor control for multi-object state-space estimation using random finite sets," *Automatica*, vol. 46, pp. 1812–1818, 2010.
- [21] B. Ristic, S. Arulampalam, and N. Gordon, *Beyond the Kalman filter: Particle filters for tracking applications*. Artech House, 2004.
- [22] T. Kailath, "The divergence and Bhattacharyya distance measures in signal selection," *IEEE Trans. Communication technology*, vol. 15, no. 1, pp. 52–60, Feb. 1967.
- [23] B. W. Silverman, *Density estimation for statistical and data analysis*. Chapman and Hall, 1986.
- [24] B. Ristic, B.-N. Vo, and D. Clark, "A note on the reward function for PHD filters with sensor control," *IEEE Trans. Aerospace and Electronic Systems*, vol. 47, no. 2, pp. 1521–1529, April 2011.